PREDICTION–BASED DIFFERENTIAL DECODING FOR RICEAN FADING CHANNELS

Lutz H.-J. Lampe and Robert Schober

Laboratorium für Nachrichtentechnik, Universität Erlangen-Nürnberg, Germany
e-mail: {LLampe,schober}@LNT.de, WWW: http://www.LNT.de/LNT2

***Abstract* — Bit-interleaved coded phase and amplitude modulation over frequency-non-selective Ricean fading channels without channel state information at the receiver is studied. We propose a low-complexity noncoherent receiver structure which is very well suited to time-variant fading transmission scenarios, and which provides gains of several dB's in power efficiency compared to conventional differential detection.**

1. INTRODUCTION

A simple, low-complexity receiver structure for noncoherent detection without channel state information (CSI) employing *hard*-decision feedback has recently been proposed by the authors [1]. This *iterative decision-feedback differential demodulation (iterative DF-DM)* has been designed for coded M-ary differential phase-shift keying (MDPSK) transmission over flat Rayleigh fading channels.

In this paper, we expand the idea of noncoherent reception with hard-decision feedback iterative decoding to general flat Ricean fading channels and bandwidth-efficient phase and amplitude modulation. As in [1], binary convolutional coding and M-ary modulation are connected via bit-interleaved coded modulation (BICM) [2, 3]. For decoding a prediction-based branch metric, cf. e.g.[4, 5, 6], is applied. The predictor structure can be excellently adjusted to the channel characteristics using standard adaptive algorithms, cf. [7, 6]. Hence, it is very well-suited to mobile communication scenarios with time-variant and possibly nonstationary transmission channels. For combined phase and amplitude modulation, we propose the application of an efficient technique using differential phase encoding and redundant amplitude modulation, which has recently been introduced in [8].

Overall, we arrive at a scheme which keeps computational complexity at a fairly low level. To assess the performance of the proposed noncoherent receiver, the achievable bit-error rate is upper bounded. Analytical and simulation results show in good agreement that generalized iterative DF-DM yields significant improvements over conventional differential demodulation for bandwidth-efficient noncoherent transmission over Ricean fading channels.

2. SYSTEM MODEL AND DECODING ALGORITHM

The block diagram of the discrete-time system model in the equivalent low-pass domain is depicted in Figure 1. The convolutional encoder output symbols are bit-wise interleaved, and $\ell \triangleq \log_2(M)$ interleaved coded bits c^μ, $0 \leq \mu \leq \ell - 1$, are mapped ($\mathcal{M}(\cdot)$) to M-ary data-carrying symbols $a[k]$ ($k \in \mathbb{Z}$: symbol discrete-time index). This is the well-known bit-interleaved coded modulation (BICM) [2, 3].

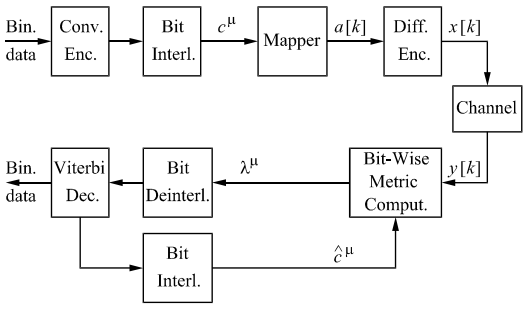

Figure 1: Discrete-time system model.

2.1. Differential Encoding and Labeling

For noncoherent demodulation the symbols $a[k]$ are usually taken from an M-ary PSK constellation $\mathcal{A} = \{\mathrm{e}^{\mathrm{j}2\pi m/M} | m = 0, 1, \ldots, M-1\}$. Then, differential encoding is done by multiplying the data-carrying symbol $a[k]$ with the previous transmit symbol $x[k-1]$ to give $x[k]$ (DPSK).

Differential amplitude and phase-shift keying (DAPSK) [9] mapping information onto both phase and amplitude changes is the straightforward extension of DPSK. Unfortunately, differential encoding of amplitudes is not suited to low-complexity iterative decoding using hard decision-feedback as explained in Section 3.2.

Therefore, another encoding strategy proposed in [8] is used. Here, the whole information is conveyed by phase increments and additionally, part of the information is also assigned to the *actual* (absolute) amplitude. The data points $a[k] \in \mathcal{A}$ are arranged in α distinct concentric rings with radii r_i, $i = 0, \ldots, \alpha-1$, and β uniformly spaced phases $\varphi_m = \frac{2\pi}{\alpha\beta}(\alpha+m)$, $m = 0, \ldots, \beta-1$, on each ring with a phase offset depending on the radius: $\mathcal{A} = \left\{ a = r_{m \bmod \alpha} \mathrm{e}^{\mathrm{j}\frac{2\pi}{\alpha\beta}m} \mid m = 0, \ldots, \alpha\beta-1 \right\}$. Clearly, $M = \alpha \cdot \beta$ is valid. Let the previous transmit symbol be $x[k-1] = r_{i[k]} \mathrm{e}^{\mathrm{j}\varphi_{n[k-1]}}$ and the differential symbol $a[k] = r_{l[k]} \mathrm{e}^{\mathrm{j}\varphi_{m[k]}}$. The operation of the differential encoder reads

$$x[k] = r_{l[k]} \mathrm{e}^{\mathrm{j}\varphi_{(n[k-1]+m[k]) \bmod \alpha\beta}} \quad . \tag{1}$$

The constellation $\mathcal{A}$ and the resulting constellation $\mathcal{X}$ of transmitted symbols is exemplary illustrated in Figure 2 for $\alpha = 2$, $\beta = 8$. Due to the redundant mapping, $\mathcal{X}$ is *expanded* and the set $\mathcal{A}$ is a true subset of $\mathcal{X}$. At any time each signal point $x \in \mathcal{X}$ is possible, which reflects the transmission diversity. Because of the appearance of the constellation $\mathcal{A}$, this differential encoding strategy is referred to as *twisted absolute*

amplitude and differential phase-shift keying (TADPSK) [8]. In order to specify certain constellations, we use the unique notation TαADβPSK, whereas for pure phase modulation ($\alpha = 1$) the usual notation MDPSK ($M \equiv \beta$) is applied. For mapping of signal points usual Gray labeling (GL) with respect to Euclidean distance is applied, which has proved to be advantageous for BICM and coherent transmission [2, 3]. In case of TADPSK, GL is separately applied to $\log_2(\alpha)$ amplitude and $\log_2(\beta)$ phase bits.

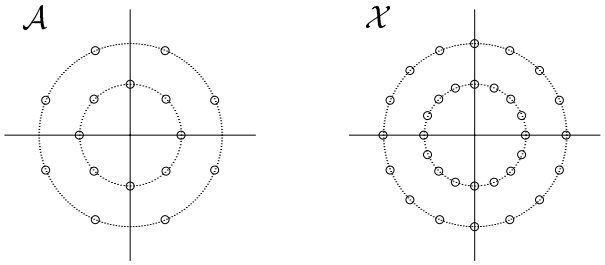

Figure 2: Signal constellations $\mathcal{A}$ and $\mathcal{X}$ for $\alpha = 2$, $\beta = 8$.

2.2. Transmit Channel

We assume sufficiently slow fading, i.e., the channel does not change significantly during one symbol interval T, and transmitter and receiver filters with square-root Nyquist characteristics. Hence, the discrete-time Ricean fading channel is frequency-non-selective (flat) and the input-output relation reads

$$y[k] = \mathrm{e}^{\mathrm{j}\theta} \cdot g[k] \cdot x[k] + n[k] \,, \tag{2}$$

where the fading process $g[\cdot]$ and the noise process $n[\cdot]$ are mutually independent correlated and uncorrelated zero-mean complex Gaussian random processes, respectively. θ represents an unknown, constant uniformly distributed phase shift. The direct component of the fading process is $g_d[k] = \mathcal{E}\{g[k]\} = \mathrm{e}^{\mathrm{j}2\pi f_D T k} g_m$, where $\mathcal{E}$ denotes expectation, f_D accounts for a Doppler shift of the direct component, and $g_m \in \mathbb{C}$ is independent of k. The scattered fading component $g_s[k] = g[k] - g_d[k]$ has variance σ_s^2, and the Ricean factor is defined as $K \triangleq \frac{|g_m|^2}{\sigma_s^2}$. Assuming appropriate normalization, $g[k]$ has unit power and $n[k]$ has variance $\sigma_n^2 = N_0/\bar{E}_s$. Here, $\bar{E}_s$ is the average received energy per symbol and N_0 is the single-sided power spectral density of the underlying continuous-time passband noise process. Finally, for the autocorrelation function of the fading process we assume the widely used Jakes fading model with one-sided bandwidth B_f.

2.3. Iterative Decoding Algorithm

At the receiver, bit branch metrics λ^μ are computed (see Section 3) and deinterleaved to give the soft input for the standard Viterbi decoder. Here, *a priori* information on the fading channel is assumed not to be available. To improve power efficiency of noncoherent demodulation, for metric calculation an increased observation interval of $N \geq 2$ consecutively received signal samples is employed. To keep computational complexity low, the metric calculation makes use of *hard* decisions $\hat{c}^\mu$ delivered from a previous decoding iteration (cf. Fig. 1). This *iterative decision-feedback differential demodulation (DF-DM)* [1] is repeated in a number of iterations.
Of course, for the first demodulation of a received sequence (first decoding iteration), no previous decisions $\hat{c}^\mu$ are available. Then, to keep the demodulation as simple as possible, we resort to *conventional differential demodulation (C-DM)* based on two consecutively received signal samples. That is, for C-DM the branch metric derived in Section 3 is applied, but with an observation interval of $N = 2$ and without application of decision feedback. However, instead of averaging over $M/2$ trial data symbols, whose labels have the same binary value at the considered bit position, only the dominant metric term is taken into account, cf. [2, 3]. In other words, only the most probable representative of the considered bit, i.e., the "nearest-neighbor" signal point, is used as trial signal point. This approach allows for further complexity reduction with negligible performance loss.
It should be mentioned that iterative hard-decision feedback decoding has also been proposed in [10] for coherent BICM, where mainly the labeling of signal points is regarded. Here, we concentrate on the performance improvement due to an prolonged observation interval.

3. Metric Calculation

Linear prediction has been successfully proposed for power efficient noncoherent detection, e.g., [4, 5, 11, 6]. Here, we apply this approach to coded (TA)DPSK with hard decision-feedback decoding.

3.1. Derivation

Taking into account the differential encoder operation (1) and defining the reference symbol

$$r_{\mathrm{ref}}[k-1] \triangleq \mathrm{e}^{\mathrm{j}\theta} \cdot g[k] \cdot x[k-1]/|x[k-1]| \,, \tag{3}$$

the channel equation (2) can be rewritten as

$$y[k] = r_{\mathrm{ref}}[k-1] \cdot a[k] + n[k] \,. \tag{4}$$

From (4) it is immediately obvious that $r_{\mathrm{ref}}[k-1]$ has to be known as precisely as possible at the receiver to approach the performance of (optimum) coherent reception. As an estimate $r_{\mathrm{e}}[k-1]$ for $r_{\mathrm{ref}}[k-1]$ we propose the output of an $(N-1)$st order linear predictor:

$$r_{\mathrm{e}}[k-1] = \sum_{\kappa=1}^{N-1} p'_\kappa[k] y[k-\kappa] \,. \tag{5}$$

Thus, overall an observation interval of N received symbols is applied for bit branch-metric computation.
For combined phase and amplitude modulation the optimum predictor with respect to the minimum mean-squared error (MMSE) criterion has to estimate a random process with time-variant autocorrelation function depending on $|x[\cdot]|$. However, this is not suitable for a practical implementation using adaptive algorithms. By treating $|x[\cdot]|$ as random variable a

(suboptimal) time-invariant solution is proposed in [12]. Following this approach for TADPSK modulation, we obtain

$$p'_\kappa[k] = p_\kappa \frac{1}{|a[k-\kappa]|} \prod_{l=1}^{\kappa-1} \frac{a[k-l]}{|a[k-l]|} \tag{6}$$

where p_κ, $1 \le \kappa \le N-1$, are the time-invariant coefficients of the $(N-1)$st order predictor for the process $g[k] + \mathrm{e}^{-\mathrm{j}\theta}\frac{n[k]}{x[k]}$.

So far, we have assumed that the transmitted symbols are known. For iterative decoding considered here, $a[k-\kappa]$, $1 \le \kappa \le N-1$, in (6) are replaced by hard decisions $\hat{a}[k-\kappa]$ from the previous decoding step. Finally, the estimated reference symbol to be used follows as

$$\hat{r}_e[k-1] = \sum_{\kappa=1}^{N-1} p_\kappa \frac{1}{|\hat{a}[k-\kappa]|} \prod_{l=1}^{\kappa-1} \frac{\hat{a}[k-l]}{|\hat{a}[k-l]|} y[k-\kappa] \ . \tag{7}$$

Having found the estimated reference symbol, we additionally apply $\ell-1$ decision-feedback bits $\hat{c}^\nu$ to specify the trial symbol $\tilde{a}[k] = \mathcal{M}(\hat{c}^0, \ldots, \hat{c}^{\mu-1}, b, \hat{c}^{\mu+1}, \ldots, \hat{c}^{\ell-1})$, $b \in \{0,1\}$, $0 \le \mu \le \ell-1$. Then, for the μth address bit of $a[k]$ the prediction-based metric

$$\lambda_b^\mu = -|y[k] - \hat{r}_e[k-1]\tilde{a}[k]|^2 \tag{8}$$

is obtained, where the subscript refers to the assumed value $c^\mu = b$. Here, we have approximated the sequence of prediction errors $y[k] - \hat{r}_e[k-1]\tilde{a}[k]$ as stationary white Gaussian random process. This assumption is necessary for analytical tractability of the problem and becomes more justified for increasing N.

3.2. Discussion

As already noted, N received signal samples are used for metric calculation. However, computational complexity is almost independent of the observation length N due to hard-decision feedback. We observe that the number of branch bit metrics λ_b^μ for DF-DM is identical to that for C-DM ($N = 2$). According to (8) and (7), calculation of the prediction-based branch metrics does not involve computationally complex operations. Of course, the predictor coefficients p_κ have to be obtained. For this purpose, the recursive least-squares (RLS) algorithm can be straightforwardly and efficiently applied [7, 6]. The predictor coefficients adjusted via the RLS-algorithm also compensate for Doppler shifts and frequency offsets [6]. Thus, prediction-based differential decoding is very well suited to practical implementation where the receiver often has to cope with nonstationary environments and statistical properties of the channel are not known *a priori*.

We also note that the determination of "nearest neighbor" signal points required for BICM with $N = 2$ and low-complexity branch metrics (see Section 2.3) is easily accomplished. Simply taking the maximum of $|y[k] - p_1 y[k-1]\tilde{a}[k]/|\tilde{a}[k-1]||^2$ (cf. (7), (8)) over α possible values $|\tilde{a}[k-1]|$ ($\alpha = 1$ for DPSK) and all $M/2$ symbols $\tilde{a}[k]$ representing the considered binary symbol gives the "nearest neighbor" $\tilde{a}[k]$ and already constitutes the branch metric.

In [13] also the ML-based bit metric utilizing an observation length N is given. Remarkably, only for pure DPSK and $K = 0$, i.e., Rayleigh fading, the ML-based and the prediction-based approach are equivalent, i.e., the ML metric can be transformed into a predictor form, cf. e.g. [4, 5, 1]. Although ML-based noncoherent reception is much more complex to implement, e.g., the modified Bessel function $I_0(\cdot)$ has to be evaluated and separate estimation of the Doppler shift f_D is required, in terms of performance the prediction-based approach is almost identical (DPSK, $\alpha = 1$) or only somewhat inferior (TADPSK, $\alpha > 1$) to the ML-based approach. This has been confirmed both by an analysis of the associated cutoff rates and by simulation results [13].

Finally, we observe that the well-known DAPSK modulation [9] is not suited to the proposed iterative decoding strategy. For DAPSK, amplitude changes instead of actual amplitudes are used to calculate the reference symbol $\hat{r}_e[k-1]$ (cf. [12, Eq. (9)]). Due to differential amplitude encoding, a single wrong amplitude decision $\hat{a}[k]$ affects all subsequent amplitude values until two erroneous decisions compensate each other. In case of uncoded DAPSK, double errors are very likely. However, in case of coded DAPSK and DF-DM, the integrator (differential amplitude encoder) necessary for remodulation after hard decision transforms a single error event into a very long error sequence. Of course, the same argument applies to pure differential phase encoding. However, since the noncoherent metric is insensitive against constant phase offsets, an erroneously fed back phase only affects decisions within one observation interval.

4. THEORETICAL ANALYSIS

In [13] the convergence of iterative DF-DM is analytically judged from the corresponding estimation error variance. It is conjectured that hard-decision feedback iterative decoding with prediction-based metrics converges for bit-error rates (BER), which are of interest in practical applications. Furthermore, from the associated cutoff rates potential gains of several dB's of iterative DF-DM with $N > 2$ over C-DM ($N = 2$) are predicted.

In this paper, we derive analytical expressions which provide tight upper bounds for the BER of *genie-aided* DF-DM, i.e., for DF-DM with error-free decision feedback, whose performance is approached by realizable DF-DM after a number of iterations.

Using the union bound for binary convolutional codes of rate $R_c = k_c/n_c$, the bit-error rate is upper bounded by

$$\mathrm{BER} \le \frac{1}{k_c} \sum_{d=1}^{\infty} W(d) f(d) \ , \tag{9}$$

where $W(d)$ is the total input weight of error events of Hamming distance d, and $f(d)$ denotes the pairwise error probability for two code words with Hamming distance d. For (9) to be valid, we assume ideal bit interleaving and symmetric BICM channels (cf. [3]).

In [3, Eq. (47)] an expurgated bound $f_{\mathrm{ex}}(d)$ for the pairwise error probability is derived, which is a true upper bound, if for each $a \in \mathcal{A}_b^\mu$ there is only one relevant error event

$\{a \rightarrow a'\}$ with $a' \in \mathcal{A}_{\bar{b}}^{\mu}$. Here, $\mathcal{A}_{\bar{b}}^{\mu}$ represents the subset of all symbols $a \in \mathcal{A}$ whose label has the value $b \in \{0,1\}$ in position μ. For the metric computation (8) with genie-aided bit-decision feedback the trial symbol $a \in \mathcal{A}_b^{\mu}$ with $a \triangleq \mathcal{M}(c^0, \ldots, c^{\mu-1}, b, c^{\mu+1}, \ldots, c^{\ell-1})$ is considered. Hence, there is only one alternative symbol $a' \in \mathcal{A}_{\bar{b}}^{\mu}$ with $a' \triangleq \mathcal{M}(c^0, \ldots, c^{\mu-1}, \bar{b}, c^{\mu+1}, \ldots, c^{\ell-1})$. Consequently, $f_{\mathrm{ex}}(d)$ can be applied to the situation at hand.
To obtain an analytical expression for $f_{\mathrm{ex}}(d)$, the difference

$$\Delta(a, a') \triangleq \lambda_b^{\mu} - \lambda_{\bar{b}}^{\mu} \tag{10}$$

between the metric for the μth bit of the true data symbol a and the alternative trial symbol a' is regarded. Using (8), (7), it is straightforward to show that $\Delta(a, a')$ can be written as

$$\Delta(a, a') = [X^* Y^*] \begin{bmatrix} 0 & C^* \\ C & B \end{bmatrix} \begin{bmatrix} X \\ Y \end{bmatrix} \triangleq \boldsymbol{z}^H \boldsymbol{F} \boldsymbol{z} \ , \tag{11}$$

where the definitions

$$X \triangleq g[k] + \mathrm{e}^{-\mathrm{j}\theta} n[k]/x[k] \tag{12}$$

$$Y \triangleq \sum_{\kappa=1}^{N-1} p_{\kappa} (g[k-\kappa] + \mathrm{e}^{-\mathrm{j}\theta} n[k-\kappa]/x[k-\kappa]) \tag{13}$$

$$C \triangleq a(a-a')^* \tag{14}$$

$$B \triangleq |a'|^2 - |a|^2 \tag{15}$$

are used. Taking the rotational invariance of $n[k]$ into account, from (13) we note that the probability density function (pdf) of $\Delta(a, a')$ depends on the amplitudes $|x[k-\kappa]| = |a[k-\kappa]|$, $1 \leq \kappa \leq N-1$. Conditioned on $|a[k-\kappa]|$, $\Delta(a, a')$ in (11) constitutes a Hermitian quadratic form of complex Gaussian distributed random variables with mean $\bar{\boldsymbol{z}} \triangleq \mathcal{E}\{\boldsymbol{z}\}$ and covariance matrix $\boldsymbol{R} \triangleq \mathcal{E}\{(\boldsymbol{z}-\bar{\boldsymbol{z}})(\boldsymbol{z}-\bar{\boldsymbol{z}})^H\}$. Thus, the Laplace transform $\Phi_{\Delta(a,a')}(s)$ of the pdf of $\Delta(a, a')$ is the average of all α^{N-1} conditioned transforms $\Phi^c_{\Delta(a,a')}(s)$, which read [14]

$$\Phi^c_{\Delta(a,a')}(s) = \frac{\exp(-s\bar{\boldsymbol{z}}^H (\boldsymbol{F}^{-1} + s\boldsymbol{R})^{-1} \bar{\boldsymbol{z}})}{\det\{\boldsymbol{I} + s\boldsymbol{R}\boldsymbol{F}\}} \ . \tag{16}$$

Here, $\boldsymbol{I}$ is the 2×2 identity matrix, and $\det\{\cdot\}$ denotes the determinant of a matrix.
Having found $\Phi_{\Delta(a,a')}(s)$, a convenient form of $f_{\mathrm{ex}}(d)$ is given as [3, Eqs. (48),(49)]

$$f_{\mathrm{ex}}(d) = \frac{1}{2\pi\mathrm{j}} \int_{v-\mathrm{j}\infty}^{v+\mathrm{j}\infty} \left(\frac{1}{\ell M} \sum_{\mu=0}^{\ell-1} \sum_{b=0}^{1} \sum_{a \in \mathcal{A}_b^{\mu}} \Phi_{\Delta(a,a')}(s) \right)^d \frac{\mathrm{d}s}{s}, \tag{17}$$

where $v > 0$ lies in the region of convergence of $\Phi_{\Delta(a,a')}(s)$. A closed-form solution for the integral in (17) may be obtained from the residues, cf. [15]. $f_{\mathrm{ex}}(d)$ (17) can be also efficiently computed based on a change of variable and Gauss-Chebyshev quadratures as shown in [16].

Applying $f_{\mathrm{ex}}(d)$ as upper bound for $f(d)$ in (9), an upper bound for the BER of genie-aided DF-DM is obtained. In accordance with the results in [3] this bound is very tight for BER's which are usually of interest.
Finally, we note that for C-DM (9) with $f_{\mathrm{ex}}(d)$ can be used as an approximation for BER. Such an approach yields good approximations for DPSK (cf. [3] for coherent PSK). However, for TADPSK and C-DM, the analytical result will underestimate the true BER, because the trial amplitude symbol $|\tilde{a}[k-1]|$ required for metric computation is supposed to be known, but feedback is unavailable. Thus, subsequently we show the respective BER's for C-DM with DPSK only.

5. RESULTS

In this section, BER's calculated according to (9) using the expurgated bound (17), and BER's obtained from simulations of the transmission system are presented as functions of $\bar{E}_b/N_0$ ($\bar{E}_b$: average energy per information bit). As interesting examples for bandwidth-efficient noncoherent transmission, we consider T2AD8PSK and alternatively 8/16DPSK with modulation rates of 2 bit/symbol and 3 bit/symbol. The ring ratio of T2AD8PSK is fixed to $r = 1.8$. For BICM, 16-state punctured convolutional codes taken from [17], randomly generated bit-interleavers, and standard Viterbi decoding are applied.
Subsequently, the BER curves for C-DM ($N = 2$) and DF-DM with $N = 3$ and $N = 5$, respectively, are shown. In case of DF-DM, for the sake of clarity only BER's obtained after 4 iterations are given. However, we would like to mention that for DPSK convergence to genie-aided DF-DM is already achieved after 2 iterations [13]. For genie-aided DF-DM, both simulated and analytical results are shown.
First, for transmission of 2 bit/symbol over Ricean fading with $10\log_{10}(K) = 3$ dB, $B_f T = 0.01$, and zero Doppler shift f_D, T2AD8PSK with $R_c = 1/2$ and 8DPSK with $R_c = 2/3$ are compared in Figure 3. Bit-interleaving corresponding to 4000 channel symbols is applied in order to provide transmission diversity. For both modulation schemes, DF-DM outperforms C-DM for BER $\lesssim 10^{-1}$ and improves significantly power efficiency of noncoherent detection. The gap to coherent transmission is considerably reduced by DF-DM with $N = 5$ for this moderate fading velocity. We further observe that T2AD8PSK with DF-DM is superior to pure phase modulation by about 1-2 dB at BER $\lesssim 10^{-4}$. Remarkably, the analytically obtained upper bounds for genie-aided DF-DM become tight for BER $\approx 10^{-3}$. Thus, system design and analysis can conveniently be done regarding bounds only.
Next, results for T2AD8PSK and 16DPSK transmission with bandwidth efficiency of 3 bit/symbol are illustrated in Figure 4. Here, the fading parameters $10\log_{10}(K) = 3$ dB, $B_f T = 0.03$, and $f_D T = 0.015$ are valid, and bit-interleaving corresponding to 2000 channel symbols is performed. Again, DF-DM with increased observation length N achieves substantial gains over conventional differential demodulation. Due to relatively fast fading assumed here, a gap of about 4 dB between improved noncoherent reception and idealized coherent reception with perfect CSI is unavoidable. For 16QAM with CSI at 14 dB BER $= 9 \cdot 10^{-6}$ is achieved. Compar-

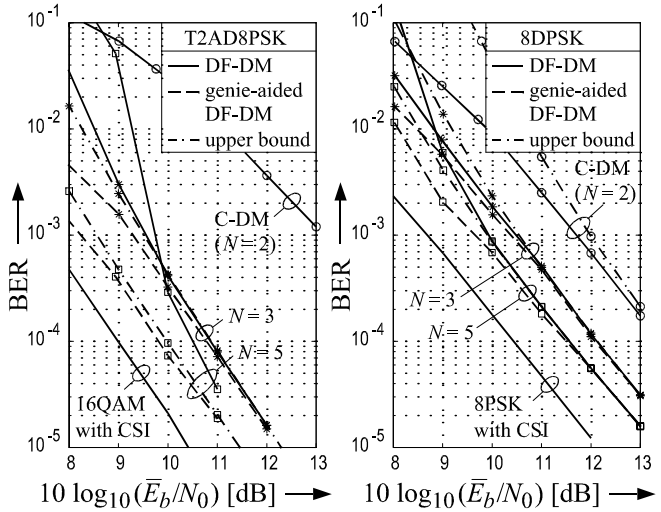

Figure 3: BER over $\bar{E}_b/N_0$. Left: T2AD8PSK. Right: 8DPSK. 2 bit/symbol over Ricean fading with $10\log_{10}(K) = 3$ dB, $B_fT = 0.01$, $f_DT = 0$. C-DM with $N = 2$ and DF-DM with 4 iterations. Dashed lines: genie-aided DF-DM. Dash-dotted lines: upper bound for genie-aided DF-DM.

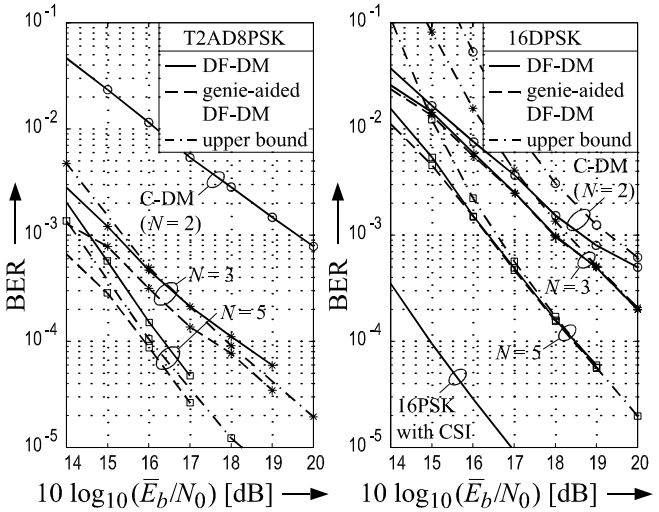

Figure 4: BER over $\bar{E}_b/N_0$. Left: T2AD8PSK. Right: 16DPSK. 3bit/symbol over Ricean fading with $10\log_{10}(K) = 3$ dB, $B_fT = 0.03$, $f_DT = 0.015$. C-DM with $N = 2$ and DF-DM with 4 iterations. Dashed lines: genie-aided DF-DM. Dash-dotted lines: upper bound for genie-aided DF-DM.

ing T2AD8PSK and 16DPSK, we observe that DF-DM with combined amplitude and phase modulation is advantageous. For BER $\lesssim 10^{-4}$, T2AD8PSK yields gains of 2-3 dB in power efficiency over 16DPSK. Finally, as both DF-DM with erroneous feedback and analytically obtained upper bounds sufficiently converge to genie-aided DF-DM, we conclude that the performance of iterative DF-DM is favorably studied based on the analytical expressions derived in Section 4.

6. Conclusions

Power- and bandwidth-efficient noncoherent transmission over flat Ricean fading channels is investigated. The presented receiver structure is perfectly suited to low-complexity implementation. An upper bound for the achievable bit-error rate of iterative DF-DM is derived, which provides a valuable instrument for system design and analysis. Analytical and simulation results show in good agreement that TADPSK modulation with prediction-based iterative DF-DM yields substantial performance improvements over DPSK with conventional differential demodulation.

References

[1] L.H.-J. Lampe and R. Schober. Iterative Decision-Feedback Differential Demodulation of Bit-Interleaved Coded MDPSK for Flat Rayleigh Fading Channels. *IEEE Trans. Com.*, 49(7):1176–1184, July 2001.

[2] E. Zehavi. 8–PSK Trellis Codes for a Rayleigh Channel. *IEEE Trans. Com.*, 40(5):873–884, May 1992.

[3] G. Caire, G. Taricco, and E. Biglieri. Bit–Interleaved Coded Modulation. *IEEE Trans. Inf. Theory*, 44:927–946, May 1998.

[4] P.Y. Kam and C.H. Teh. Reception of PSK Signals Over Fading Channels Via Quadrature Amplitude Estimation. *IEEE Trans. Com.*, 31:1024–1027, August 1983.

[5] J. H. Lodge and M. L. Moher. Maximum Likelihood Sequence Estimation of CPM Signals Transmitted Over Rayleigh Flat–Fading Channel. *IEEE Trans. Com.*, 38:787–794, June 1990.

[6] R. Schober and W.H. Gerstacker. Decision–Feedback Differential Detection Based on Linear Prediction for MDPSK Signals Transmitted over Ricean Fading Channels. *IEEE J. Select. Areas Commun.*, 18:391–402, March 2000.

[7] R.J. Young and J.H. Lodge. Detection of CPM Signals in Fast Rayleigh Flat–Fading Using Adaptive Channel Estimation. *IEEE Trans. Veh. Tech.*, pages 338–347, May 1995.

[8] L.H.-J. Lampe, R.F.H. Fischer, and J.B. Huber. Differential Phase Shift Keying with Constellation Expansion Diversity. In *Proceedings ISIT*, page 136, Sorento, Italy, June 2000.

[9] W.T. Webb, L. Hanzo, and R. Steele. Bandwidth Efficient QAM Schemes for Rayleigh Fading Channels. *IEE Proceedings–I*, 138(3):169–175, June 1991.

[10] X. Li and J.A. Ritcey. Trellis–Coded Modulation with Bit Interleaving and Iterative Decoding. *IEEE J. Select. Areas Commun.*, 17(4):715–724, April 1999.

[11] P. Hoeher and J. Lodge. "Turbo DPSK": Iterative Differential PSK Demodulation and Channel Decoding. *IEEE Trans. Com.*, 47(6):837–843, June 1999.

[12] R. Schober, W.H. Gerstacker, and J.B. Huber. Decision–Feedback Differential Detection for 16DAPSK Transmitted over Ricean Fading Channels. In *Proceedings VTC*, pages 2515–2519, Amsterdam, September 1999.

[13] L.H.-J. Lampe and R. Schober. Low-Complexity Iterative Demodulation for Noncoherent Coded Transmission over Ricean Fading Channels. *In revision: IEEE Trans. Veh. Techn., 2000*.

[14] M. Schwartz, W. Bennett, and S. Stein. *Communication Systems and Techniques*. McGraw–Hill, New York, 1966.

[15] J.K. Cavers and P. Ho. Analysis of the Error Performance of Trellis–Coded Modulations in Rayleigh–Fading Channels. *IEEE Trans. Com.*, 40:74–83, January 1992.

[16] E. Biglieri, G. Caire, G. Taricco, and J. Ventura-Traveset. Computing Error Probabilities over Fading Channels: A Unified Approach. *Europ.Trans. Telecom.*, 9:15–25, Jan/Feb 1998.

[17] J.B. Huber. *Trelliscodierung*. Springer–Verlag, Berlin, 1992.